Predicting Inter-Hemispheric Transfer Time from the Diffusion Properties of the Corpus Callosum in Healthy Individuals and Schizophrenia Patients: A Combined ERP and DTI Study

Thomas J. Whitford[1,2,3,4,*], **Marek Kubicki**[1,2,4], **Shahab Ghorashi**[2,4], **Jason S. Schneiderman**[1,4], **Kathryn J. Hawley**[1,4], **Robert W. McCarley**[2,4], **Martha E. Shenton**[1,2,4,†], and **Kevin M. Spencer**[2,4,†]

[1] Psychiatry Neuroimaging Laboratory, Brigham and Women's Hospital, MA, USA

[2] Veterans Affairs Boston Healthcare System, MA, USA

[3] Melbourne Neuropsychiatry Centre, Department of Psychiatry, University of Melbourne and Melbourne Health, VIC, Australia

[4] Department of Psychiatry, Harvard Medical School, MA, USA

Abstract

Background—Several theories of schizophrenia have emphasized the role of aberrant neural timing in the etiology of the disease, possibly as a consequence of conduction delays caused by structural damage to the white-matter fasciculi. Consistent with this theory, increased inter-hemispheric transmission times (IHTTs) to unilaterally-presented visual stimuli have been reported in patients with schizophrenia. The present study investigated whether or not these IHTT abnormalities could be underpinned by structural damage to the visual fibers of the corpus callosum.

Methods—30 schizophrenia patients and 22 matched controls underwent Event Related Potential (ERP) recording, and a subset of 19 patients and 16 controls also underwent 3T Diffusion-Tensor Imaging (DTI). Unilateral visual stimuli (squares, 2×2 degrees) were presented 6 degrees lateral to either side of a central fixation point. IHTTs (ipsilateral minus contralateral latencies) were calculated for the P1 and N1 components at occipital-temporal sites in current source density-transformed ERPs. The visual fibers of the corpus callosum were extracted with streamline tractography and the diffusion metrics of Fractional Anisotropy (FA) and Mode calculated.

Results—While both subject groups exhibited highly significant IHTTs across a range of posterior electrode pairs, and significantly shorter IHTTs from left-to-right hemisphere than vice versa, no significant groupwise differences in IHTT were observed. However, participants' IHTTs were linearly related to their FA and Mode, with longer IHTTs being associated with lower FA and more prolate diffusion ellipsoids.

[*]Corresponding Author: Thomas J. Whitford, Psychiatry Neuroimaging Laboratory, Brigham and Women's Hospital, Harvard Medical School, 1249 Boylston St, Boston, MA, 02215, USA, Phone: +1 617 525 6119, Fax: +1 617 525 6150, whitford@bwh.harvard.edu.
[†]Denotes equal last authorship

Conclusions—These results suggest that IHTTs are estimable from DTI measures of white matter integrity. In light of the range of diffusion abnormalities that have been reported in patients with schizophrenia, particularly in frontal fasciculi, these results support the conjecture that schizophrenia is ultimately underpinned by abnormalities in neural timing.

Keywords

Event Related Potential; Diffusion Tensor Imaging; Fractional Anisotropy; conduction velocity; connectivity

1. Introduction

A unifying tenet of the 'connectivity' theories of schizophrenia is that the disease is ultimately underpinned by abnormal interactions *between* brain regions, as opposed to abnormal brain regions *per se* (Friston, 1998). Several 'connectivity' theories have emphasized the role of aberrant neural timing in the etiology of schizophrenia (Andreasen et al., 1999; Bartzokis, 2002; Bressler, 2003; Phillips and Silverstein, 2003; Stephan et al., 2009). It has been suggested that this aberrant neural timing could be caused by conduction delays arising from structural damage to the white-matter fasciculi that physically connect spatially disparate populations of neurons (Bartzokis, 2002; Fields, 2008; Whitford et al., 2010a). This suggestion is supported by the facts that a) a primary role of myelin is to increase the speed of neural transmissions (Baumann and Pham-Dinh, 2001), b) damage to the white-matter has consistently been shown to cause conduction delays or even blockages *in vivo*, such as characteristically occurs in multiple sclerosis patients with optic neuritis (Cuypers et al., 1995), and c) schizophrenia patients have repeatedly been shown to exhibit white-matter abnormalities, both *in vitro* with microscopy (Uranova et al., 2007) and *in vivo* with structural MRI (Whitford et al., 2007) and, more recently, Diffusion-Tensor Imaging (DTI) (Kubicki et al., 2007). Thus there is reason to suspect that schizophrenia is associated with neural conduction delays caused by structural damage to white-matter fasciculi.

While obtaining an accurate estimate of neural conduction velocities *in vivo* in the human central nervous system is problematic without the use of invasive intra-cranial electrodes, several previous studies have used electroencephalography (EEG) to estimate inter-hemispheric transmission time (IHTT) from the event-related potentials (ERPs) evoked by unilaterally-presented visual stimuli (Brown and Jeeves, 1993; Moes et al., 2007; Nowicka et al., 1996; Saron and Davidson, 1989). IHTT has typically been calculated as the latency of an early ERP component (e.g., P1 or N1) measured at a posterior electrode site over the cerebral hemisphere contralateral to the visual stimulus (e.g., PO8 for a left-visual field stimulus) subtracted from the latency of the component measured at the homologous electrode site over the hemisphere ipsilateral to the stimulus (i.e., PO7 in this example). IHTT is an attractive measure for investigating the integrity of fiber tracts *in vivo* because its anatomical substrate, the visual fibers of the corpus callosum, is well-characterized. Visual stimuli are more commonly used than auditory stimuli in IHTT research because of the fact that in the auditory system, in contrast to the visual system, much of the inter-hemispheric transfer occurs prior to reaching primary sensory cortex (Kandel et al., 2000).

There is some ERP evidence to suggest that schizophrenia patients exhibit abnormally long IHTTs to unilaterally-presented visual stimuli (Barnett et al., 2005; Barnett and Kirk, 2005; Endrass et al., 2002). If these IHTT abnormalities are indeed underpinned by physical damage to the white-matter fibers connecting the visual cortices bilaterally, then schizophrenia patients might be expected to show DTI abnormalities in the visual fibers of the corpus callosum. However, while a number of studies have identified diffusion abnormalities in the splenium of the corpus callosum (Cheung et al., 2008; Foong et al.,

2000), including in fist-episode, antipsychotic-naïve patients (Gasparotti et al., 2009), there have been no studies (to our knowledge) that have either used DTI to investigate the structural integrity of the visual callosal fibers explicitly in schizophrenia patients, or have investigated the relationship between IHTT and the integrity of the visual callosum fibers in schizophrenia patients. Indeed, despite the established qualitative relationship between the integrity of the corpus callosum and interhemispheric transfer, as evidenced by the IHTT abnormalities exhibited by acallosal individuals; (Bayard et al., 2004), only one previous study (to our knowledge) has directly investigated their empirical relationship in healthy individuals. Westerhausen et al. (2006) estimated IHTT on the basis of the difference in P1-latency at electrodes O1 and O2 to unilaterally-presented visual stimuli, and paradoxically found that IHTT was *negatively* correlated with Mean Diffusivity in the splenium of the corpus callosum.

The present study had three primary aims. The first aim was to investigate the existence and extent of IHTT abnormalities to unilaterally-presented visual stimuli in patients with schizophrenia with a more rigorous methodology than has been employed previously, including using a dense electrode array, calculating IHTTs from multiple electrode pairs, and using Current-Source Density (CSD) transformed data. CSD (Perrin et al., 1987) is an improvement over using traditional voltage ERP measurements for estimating IHTT because it attenuates the effects of volume conduction and acts as a high-pass spatial filter, thus reducing the overlap between ERPs at contra- and ipsilateral electrode sites (Saron et al., 2003). Also, CSD is reference-independent, meaning that the waveforms at different electrodes are not influenced by activity at a common reference electrode.

The second aim was to use fiber tractography in conjunction with DTI to a) precisely extract the visual fibers of the corpus callosum, and b) quantify their structural integrity on the basis of two complementary diffusion indices, namely Fractional Anisotropy (FA) and Mode. While the majority of previous DTI studies have quantified fiber integrity solely on the basis of FA (which is an index of the asphericity of diffusion), FA cannot, as noted by Hasan (2006), determine the morphological underpinnings of this asphericity. FA, for example, is unable to distinguish between prolate diffusion (i.e., shaped like a cigar) and oblate diffusion (i.e., shaped like a pancake), despite their presumably different physiological bases. To distinguish between these scenarios, a diffusion index such as Mode is required (Ennis and Kindlmann, 2006), and hence the present study used both FA and Mode to quantify the structural integrity of the visual fibers of the corpus callosum.

The third aim of the present study was to investigate the empirical relationship between neural conduction velocity (as estimated by IHTT) and the structural integrity of the conducting fibers (as quantified by the FA and Mode of the visual callosum fibers) in healthy individuals and schizophrenia patients. By elucidating this relationship, we hoped to shed light on whether schizophrenia could feasibly be associated with subtle conduction delays causing irregularities in the precise timing of neural discharges and consequent abnormalities in neural coherence (Fries, 2005; Spencer et al., 2003).

2. Methods

2.1 Participants

Thirty-three patients with chronic schizophrenia (SZ) and 20 healthy control participants (HC) underwent EEG recordings. The SZ participants were recruited from out-patient, in-patient, day treatment and foster care programs at the Veterans Affairs Boston Healthcare System. Diagnosis of schizophrenia was made on the basis of the Structured Clinical Interview for DSM-IV (First et al., 1997), and a review of the medical record. The HC participants were recruited from the general community, and matched to the patients on age,

handedness (Oldfield, 1971), parental socioeconomic status (Hollingshead, 1965), and estimated premorbid intelligence, as assessed by performance on the Reading scale of Wide Range Achievement Test (WRAT-3) (Wilkinson, 1993). A subset of 19 SZ and 16 HC participants also underwent Diffusion-Tensor Imaging (DTI). The demographic details for the SZ and HC participants (i.e., either in both the EEG and DTI components, or in the EEG component alone) are summarized in Table 1.

Exclusion criteria for all participants were left-handedness, a history of electroconvulsive shock therapy, a history of neurological illness including epilepsy, a lifetime history of substance dependence or a history of substance abuse within the past 5 years, a history of steroid use, and estimated premorbid intelligence quotient below 75. Furthermore, HC participants were screened for the presence of an Axis-I disorder using the SCID-Non-Patient edition (First et al., 2002), and were also excluded if they reported having first-degree relative with an Axis I disorder.

The study was approved by the Institutional Review Boards of the VA Boston Healthcare System, Brigham and Women's Hospital, and Harvard Medical School. After a detailed description of the study, each subject gave written informed consent to participate.

2.2 Stimuli and Task

Participants were seated in a quiet, dimly-lit room, 1 m in front of a computer monitor on which the visual stimuli were presented. The visual stimuli consisted of a series of unilaterally-presented white squares on a black background. The squares (of visual angle 2×2 degrees) were presented for 82 ms on the horizontal meridian, with the inner edge of the squares 6.79 degrees lateral to a central fixation cross (see Figs. 1a and 1b). The fixation cross was continually present during each block of trials. On target trials, a red dot (0.82 degrees wide) was presented at fixation simultaneously with the lateral square (see Figs. 1c and 1d). Participants were instructed to maintain their gaze on the central fixation cross and count the number of targets they saw. There were 4 blocks of trials, each consisting of 30 left visual field (LVF) non-target trials, 30 right visual field (RVF) non-target trials, 8 LVF/ target trials and 7 RVF/target trials, presented in pseudo-random order. Stimulus onset asynchrony was 624 ms. Each block took approximately 1 minute to complete. Participants' data were not analyzed further if they missed 4 or more targets in one or more of the 4 blocks.

2.3 EEG Acquisition

The EEG was recorded with a Biosemi Active-Two system using sintered Ag/Ag-Cl electrodes in an electrode cap at 71 standard scalp sites (DC–100 Hz bandpass filter, 512 Hz digitization rate). The DC offsets were kept below 25 mV. During data acquisition, all channels were referred to the system's internal loop (CMS/DRL sensors located in the parietal region) and offline re-referenced to the left mastoid electrode. The bipolar vertical electro-oculogram (EOG) was derived from electrode Fp1 and an electrode below the left eye. The horizontal EOG was derived from electrodes on the left and right outer canthi.

2.4 EEG Analysis

The epoching of the EEG data was performed with BrainVision Analyzer 2.0 (Brain Products GmbH). For each of the 300 trials presented to each participant, a 1 s epoch was extracted from 405 ms pre-stimulus to 595 ms post-stimulus. Further processing was performed using the Independent Components Analysis (ICA) Toolbox (Makeig et al., 1996) in Matlab (Mathworks, Inc.) and with custom software in IDL (ITT Visual Information Solutions). ICA was used to remove ocular and other artifacts. The single trial epochs for each subject were submitted to ICA, which typically resulted in an IC that

accounted for eye blink artifact, and sometimes other ICs that accounted for other artifacts such as muscle artifacts. Artifact ICs were identified based on their characteristic topographies, time courses, and frequency distributions. The activations of the artifact ICs were set to zero and an inverse transformation was performed to return the single trial data to the voltage domain, minus the artifacts. The artifact criteria were: 1) > +/− 90 μV change in one time point; 2) amplitude range within an epoch exceeding 200 μV; and 3) horizontal EOG deviations exceeding calibration values for 1 degree of visual angle. Participants' data were not included in the data set if they had less than 200 epochs following artifact removal. The number of epochs retained per subject was (mean +/− standard deviation) 276 +/− 27 for HC and 271 +/− 21 for SZ. Only non-target trials were analyzed. Average ERPs were computed from the single-trial epochs for the LVF and RVF stimulus trials and transformed into CSD waveforms (Perrin et al., 1989) using the CSD Toolbox version 1.0 (Kayser and Tenke, 2006) (http://psychophysiology.cpmc.columbia.edu/Software/CSDtoolbox). Each participant's CSD waveforms were filtered from 1–15 Hz and baseline-corrected with a −100 to 0 ms baseline. The filter was of finite impulse response type, zero phase shift, with a 200 ms width, and passband weights determined in the frequency domain (Cook and Miller, 1992). The filter was applied to the waveforms beginning at −200 ms so that the first filtered point was −100 ms. A peak-picking algorithm was used to identify the P1 and N1 ERP components based on changes in the slope (first derivative) of the waveform. The search windows for the P1 and N1 were selected based on the grand average CSD waveforms. The P1 peak was defined as the most positive CSD value from 75–200 ms, and the N1 peak was identified as the most negative CSD value from 125–225 ms. The P1 and N1 peaks were measured at the electrode sites at which they were maximal (P1: P7/P8, P9/P10, PO7/PO8, PO9/PO10; N1: P5/P6, P7/P8, PO7/PO8, PO9/PO10). A schematic of the electrode pairs used in the P1 and N1 analyses, which were also the electrodes from which IHTT was subsequently calculated (described in section 2.7.3), is provided in Fig. 2.

2.5 DTI Acquisition

Diffusion-weighted images (DWIs) were collected on 3 Tesla GE Echospeed system (General Electric Medical Systems, Milwaukee, WI). DWIs were acquired using an echo-planar imaging sequence, and a double echo option to reduce eddy-current related distortions. To reduce impact of EPI spatial distortion, an 8-Channel coil and ASSET (Array Spatial Sensitivity Encoding techniques, GE) with a SENSE-factor (speed-up) of 2 was used. Eighty-five axial slices parallel to the AC-PC line covering whole brain were acquired, in 51 diffusion directions with b=900 s/mm^2. 8 baseline scans with b=0 were also acquired. The scan parameters were: TR 17000 ms, TE 78 ms, FOV 24 cm, 144×144 matrix, 1.7 mm slice thickness, producing isotropic 1.7×1.7×1.7 mm voxels. The total scanning time was approximately 17 minutes.

2.6 DTI Analysis

All DTI analysis was performed with the 3D-Slicer software package (http://www.slicer.org, Surgical Planning Laboratory, Brigham and Women's Hospital, Boston, Massachusetts). The splenium was manually defined on the midsagittal slice and the two neighboring sagittal slices on each participant's FA image (Fig. 3a). The voxels defined by this Region-of-Interest (ROI) were then used as seed voxels for deterministic (streamline) tractography. Streamline tractography followed the direction defined by the principal eigenvector, based on a Runge-Kutta second-order protocol, with a fixed step size of 1.5 mm. Tractography terminated upon reaching a voxel of FA<0.25 (the stopping criterion), and a length criterion was also employed whereby fibers were excluded if they were shorter than 20 mm.

To ensure that only the visual fibers of the corpus callosum were extracted, one exclusion and one inclusion ROI were introduced, i.e., fibers were excluded if they passed through the

exclusion ROI or if they did not pass through the inclusion ROI. The inclusion ROI (coronal) was placed through the posterior edge of the parieto-occipital sulcus, so as to exclude fibers that did not project posteriorly from the corpus, such as temporal callosal fibers (Fig. 3b). The exclusion ROI (axial) was placed on the dorsal-most slice of the corpus callosum, so as to exclude fibers that projected dorsally to the parietal cortex (Fig. 3b). The remaining fibers connected the primary and secondary visual cortices bilaterally (see Fig. 3c and 3d).

After extraction of the visual callosal fibers, a binary label-map was generated for each participant by labeling those voxels through which any fibers passed. FA was calculated for each voxel as per the algorithm of Basser and Pierpaoli (1996), and mean FA was calculated by averaging the FA values of the constituent voxels of the label-map. Mode was calculated for each voxel as per the algorithm of Ennis and Kindlmann (2006), and average Mode was calculated in the same way as average FA. Mode is an index of the three-dimensional shape of the diffusion ellipsoid. Specifically, Mode describes whether the diffusion ellipsoid is prolate (i.e., shaped like a cigar, and associated with a Mode ~ 1) or oblate (i.e., shaped like a pancake, and associated with a Mode ~ −1). FA and Mode are mathematically orthogonal, and two tensors with identical FA (i.e., equally aspherical) can have very different three-dimensional shapes (Ennis and Kindlmann, 2006).

2.7 Statistical Analysis

2.7.1 ERP Data
A repeated measures ANOVA was used for the analysis of the amplitude and latency of the P1 and N1 components. Visual Field (LVF vs. RVF), Hemisphere (electrodes contra- vs. ipsilateral to the stimuli), and Electrode (4 pairs, see above in EEG Analysis) were entered in the analysis as within-subjects factors, and Diagnosis (SZ vs. HC) was entered as a between-subjects factor.

2.7.2 DTI Data
Independent-samples t-tests were used to investigate for between-group differences in the FA and Mode of the visual fibers of the corpus callosum.

2.7.3 Relationship between IHTT and FA/Mode in the visual corpus fibers
IHTT was calculated for each of the 4 electrode pairs for both P1 and N1 by subtracting the latency of the component peak measured at the electrode contralateral to the visual stimulus from the latency of the component peak measured at the electrode ipsilateral to the stimulus. Linear regression was used to investigate whether it was possible to predict a participant's IHTT at each of the 4 electrode pairs (i.e., the response variable) on the basis of a linear combination of the FA and Mode of their visual corpus fibers (i.e., the predictor variables). The conservative Bonferroni correction for multiple comparisons was used to control for alpha inflation. Given the 4 electrode pairs and 2 ERP components, alpha was set to $0.05/8 = 0.00625$.

3. Results

The grand averaged CSD waveforms recorded at electrode-pair P7/P8 in response to LVF and RVF stimuli in the SZ patients and HCs are presented in Fig. 4. The P7 and P8 electrode sites were chosen for display as they exhibited among the largest P1 and N1 amplitudes to both contralateral and ipsilateral stimuli. Headmaps showing the amplitude topography of the P1 and N1 components are presented in Fig. 5.

3.1 P1 Amplitude

The main effect of Diagnosis was not significant ($F_{1,51}=0.001$, p=0.985), indicating that SZ and HC did not differ in P1 amplitude. There was a main effect of Hemisphere

($F_{1,51}$=16.986, p<0.001), indicating that electrodes contralateral to the visual stimuli had larger P1 amplitudes than ipsilateral electrodes, as expected. This effect did not differ between groups (Diagnosis × Hemisphere interaction: $F_{1,51}$=2.355, p=0.131). There was also a main effect of Electrode ($F_{3,153}$=7.742, p=0.001), indicating that the 4 electrode pairs differed in terms of their P1 amplitude. No other significant main effects or interactions were found.

3.2 P1 Latency

P1 latency did not differ between HC and SZ (Diagnosis: $F_{1,51}$=0.174, p=0.678). There was a main effect of Hemisphere ($F_{1,51}$=33.781, p<0.001), indicating that P1 latency was longer at electrodes ipsilateral vs. contralateral to the stimuli (see Fig. 6a). Significant IHTTs were also observed in both the SZ patients ($F_{1,33}$=23.364, p<0.001) and the HCs ($F_{1,19}$=14.064, p=0.001) when the groups were considered separately. However, there was no Diagnosis × Hemisphere interaction ($F_{1,51}$=0.174, p=0.678), demonstrating that IHTTs did not significantly differ between groups (Fig. 6b). A significant VF × Hemisphere interaction was observed ($F_{1,51}$=4.939, p=0.031) (Fig. 6c). Inspection of the data revealed that this was due to the IHTT from left-to-right hemisphere being shorter than IHTT from right-to-left hemisphere, across electrode pairs. There was a main effect of Electrode ($F_{3,153}$=11.865, p<0.001), indicating that the 4 electrode pairs differed in terms of their P1 latency. No other significant main effects or interactions were found. In particular, there was no Diagnosis × VF × Hemisphere interaction ($F_{1,51}$=0.122, p=0.728) indicating that the pattern of faster transfer from left-to-right hemisphere than vice versa was similar between SZ and HC.

3.3 N1 Amplitude

N1 amplitude did not differ between HC and SZ ($F_{1,51}$=0.025, p=0.876). As for P1 amplitude, a main effect of Hemisphere ($F_{1,51}$=46.187, P<0.001) was found, indicating that N1 amplitude was greater over contralateral than ipsilateral electrodes, as expected. However, again as for P1 amplitude, there was no significant Diagnosis × Hemisphere interaction ($F_{1,51}$=1.498, p=0.227). There was a significant main effect of Electrode ($F_{3,153}$=12.364, p<0.001), and there was also a significant Electrode × Hemisphere interaction ($F_{3,153}$=5.960, p=0.001), indicating that the electrode pairs differed in terms of the magnitude of the N1 contralaterality effect, which was maximal at the PO7/PO8 electrode pair and minimal at the PO9/PO10 electrode pair The Diagnosis × Electrode interaction was also significant ($F_{3,153}$=3.368, p=0.014), which was primarily due to the SZ showing non-significantly decreased N1 amplitudes at the P5/P6 electrode pair ($F_{1,51}$=2.230, p=0.142) but non-significantly increased N1 amplitudes at the PO9/PO10 electrode pair ($F_{1,51}$=1.709, p=0.197), relative to the HC. There were no other significant main effects or interactions.

3.4 N1 Latency

N1 latency did not differ between groups ($F_{1,51}$=0.042, p=0.839). There was a main effect of Hemisphere ($F_{1,51}$=62.451, p<0.001), demonstrating that N1 latency was longer at electrodes ipsilateral vs. contralateral to the stimuli (see Fig. 7a). Significant IHTTs were also observed in both the SZ patients ($F_{1,33}$=28.481, p<0.001) and the HCs ($F_{1,19}$=13.763, p=0.001) when the groups were considered separately. The Diagnosis × Hemisphere interaction was not significant ($F_{1,51}$=3.132, p=0.083), indicating that IHTTs did not differ between SZ and HC (see Fig. 7b). In contrast to the P1 results, there was no VF × Hemisphere interaction for the N1 ($F_{1,51}$=2.342, p=0.132), indicating that the IHTTs for left-to-right transfer did not differ from the IHTTs for right-to-left transfer (see Fig. 7c). Nor was the Diagnosis × VF × Hemisphere interaction significant ($F_{3,153}$=0.573, p=0.633). There was a main effect of Electrode ($F_{3,153}$=5.314, p=0.002) but there was no Electrode ×

Hemisphere interaction ($F_{3,153}$=0.153, p=0.928). There were no other significant main effects or interactions.

3.5 DTI

No significant differences were observed between SZ and HC in terms of either their FA (t(33)=0.001, p=0.99) or Mode (t(33)=0.317, p=0.754) in the visual fibers of the corpus callosum (see Fig. 8).

3.6 Relationship between IHTT and FA/Mode of the visual callosal fibers

A linear combination of the mean FA and Mode of the visual fibers of the corpus callosum accounted for a significant proportion (28.5%) of the variance in IHTT across both groups combined, when IHTT was estimated on the basis of P1 asymmetry measured from the P9/P10 electrode pair (Fig. 9).

$$IHTT(P9/P10) = -283^*FA + 72^*Mode + 93, (R^2 = 0.285, F_{2,34} = 6.391\ p = 0.005)$$

To control for the possibility of the regression being driven by between-group differences in IHTT and/or the diffusion measures, the Group × FA and Group × Mode interaction terms were added to the model. Adding these interaction terms did not significantly increase the amount of variance accounted for by the model, indicating that the relationship between IHTT and FA/Mode was comparable between the patient and control groups. Consistent with this finding, the regression model was similar and remained statistically significant when the HCs were considered alone:

$$IHTT(P9/P10) = -277^*FA + 107^*Mode + 72, R^2 = .383, F_{2,15} = 4.032\ p = 0.043.$$

Similarly, the regression model was similar and remained statistically significant when the SZ patients were considered alone.

$$IHTT(P9/P10) = -329^*FA + 44^*Mode + 180, R^2 = .317, F_{2,18} = 3.721,\ p = 0.047.$$

The correlation between IHTT and FA (alone) was highly significant for both groups combined (r(35)=−.502, p=.002), and was also significant when the control participants (r(19)=−.557, p=.013) and schizophrenia participants (r(16)=−.513, p=.042) were considered separately. A significant positive correlation was also observed across groups between FA and Mode (r(35)=.551, p=.001), which raised the issue of multicollinearity in the regression model. However, the Variance Inflation Factor (VIF) associated with the model was 1.436, which is well within the limits for acceptable multicollinearity outlined by Myers (1990).

In order to control for the possibility that the observed association between FA/Mode and IHTT was driven by variations in age and gender, we entered these variables into the regression model as nuisance covariates. The resulting model:

$$IHTT(P9/10) = -274^*FA + 92^*Mode + .62^*Age + 14.7^*Gender$$

accounted for a significant proportion (36.8%) of the variance in IHTT ($F_{4,33}=4.224$, $p=0.008$). Gender was the weakest predictor variable ($\beta=.12$, $p=.425$), and dropping it did not result in a significant reduction in the amount of variance accounted for by the model (R^2-change=.014, Fchange$_{1,29}=.654$, $p=.425$). The revised model:

$$IHTT(P9/10)= -276^*FA+87^*Mode+.62^*Age$$

accounted for 35.4% of the variance in IHTT ($F_{3,33}=5.478$, $p=.004$). To control for the possibility that the observed association between IHTT and FA/Mode was driven by within-subject variations in fiber length or fiber curvature, we calculated indices for these two variables and entered them into the regression analysis. Average fiber length was calculated by integrating the distance between consecutive points on each of the tractography-defined visual callosal fibers, and averaging over all fibers. Mean curvature for each fiber was calculated by integrating the inverse of the radius of the osculating circle along the fiber and dividing by the fiber length. Average curvature for the entire bundle was then calculated by averaging the mean curvature of each fiber. Adding these variables did not significantly augment the amount of variance accounted for by the model (R^2-change = 0.008, $F_{2,29}=.168$, $p=.846$), and the revised model remained significant when these variables were included ($F_{4,33}=3.036$, $p=.033$), indicating that the observed association between IHTT and FA/Mode was not being driven by within-subject variations in fiber length or fiber curvature.

After Bonferroni correction, FA and Mode did not account for a significant proportion of the variance in IHTT when IHTT was estimated on the basis of the P1 latency asymmetry at the other three electrode pairs at which P1 was maximal (P7/P8: $F_{2,34}=.518$, $p=.601$; PO7/PO8: $F_{2,34}=1.630$, $p=.212$; PO9/PO10: $F_{2,34}=.680$, $p=.514$). When IHTT was estimated on the basis of the average of the P1 latencies calculated at each of the four electrode pairs, however, FA and Mode accounted for a near-significant proportion of the variance in IHTT ($F_{3,34}=2.84$, $p=.054$, controlling for age). FA and Mode did not account for a significant proportion of the variance in IHTT when IHTT was estimated on the basis of the N1 latency asymmetry at four electrode pairs at which N1 was maximal (P5/P6: $F_{2,34}=.493$, $p=.615$; P7/P8: $F_{2,34}=.213$, $p=.809$, PO7/PO8: $F_{2,34}=.318$, $p=.73$; PO9/PO10: $F_{2,34}=.344$, $p=.711$).

4. Discussion

There were five main findings in the present study:

1. Both SZ and HC exhibited highly significant differences ($p<0.001$) in the latency of both the P1 and N1 components to unilaterally-presented visual stimuli at ipsilateral as opposed to contralateral electrode sites. In other words, highly significant IHTTs (of around 10 ms for P1 and 15 ms for N1) were observed in both participant groups.

2. Significantly longer IHTTs (estimated from P1) were observed, in both groups, for stimuli presented in the left visual field compared to those presented in the right visual field. In other words, inter-hemispheric transfer from the left-to-the-right hemisphere was shorter than from the right-to-the-left.

3. There were no significant differences in IHTT (calculated from either P1 or N1) between SZ and HC.

4. There were no significant differences between SZ and HC participants in terms of the diffusion properties of the visual fibers of the corpus callosum, as measured with FA and Mode.

5. Linear regression analysis revealed a predictable relationship between participants' IHTTs and the diffusion properties (i.e., FA and Mode) of their visual corpus fibers, such that participants with the lowest FA and highest Mode (i.e., most prolate diffusion ellipsoids) exhibited the longest IHTTs. In light of the fact that schizophrenia patients have consistently been shown to have subnormal levels of FA in numerous white-matter fasciculi (especially those projecting from the frontal lobe, such as the uncinate fasciculus, arcuate fasciculus and cingulum bundle (Kubicki et al., 2007; Whitford et al., in press)), the results of the linear regression suggest that schizophrenia may be associated with conduction delays along these fasciculi. Considering the deleterious effects that such conduction delays might be expected to have on neural coherence (Fries, 2005), this possibility has significant implications for the prevailing connectivity theories of schizophrenia.

The estimated magnitude of the IHTT did not differ significantly between the four electrode pairs for either P1 (average 10 ms, ranging from 14 ms to 24 ms) or N1 (average 15 ms, with a range of 14 to 17 ms) (see Figs. 6 and 7). These estimates are similar to the IHTTs reported for both P1 (Saron and Davidson, 1989) and N1 (Moes et al., 2007; Saron and Davidson, 1989) in previous ERP studies, illustrating the reliability of the basic approach. Our finding of asymmetric IHTTs to in response to LVF as opposed to RVF stimuli has been reported in several previous ERP studies, although the direction of these asymmetries has been inconsistent. For example, while Nowicka, Grabowska and Fersten (1996) reported faster transfer from left-to-right hemisphere to visual gratings (consistent with the results of the present study), both Saron and Davidson (1989) and (Patston et al., 2007) observed faster transfer from right-to-left hemisphere for similar stimuli. The microstructural underpinnings of these IHTT asymmetries are unclear and represent a point of contention in the literature. Marzi (1991), for example, has argued that these asymmetries are underpinned by differences in the number of corpus axons projecting from the left hemisphere to the right and vice versa. In contrast, both Braun (1992) and Nowicka, Grabowska and Fersten (1996) have suggested that while both hemispheres contain comparable numbers of fast and slow-conducting callosal fibers, the brain has evolved to ensure "the fast transmission of information to the hemisphere which is more efficient in its processing [of the particular stimulus]" (Nowicka, Grabowska and Fersten, 1996, p147). Regardless of their physiological bases, the asymmetric IHTTs observed in the present study provide further evidence that cerebral lateralization is not limited to language-related functions, but instead occurs in a variety of sensorimotor and cognitive processes.

As illustrated in Figs. 6b and 7b, there were no significant differences between the SZ and HC participants in terms of their IHTTs. Furthermore, there were no significant Diagnosis × VF × Hemisphere interactions, indicating that both groups exhibited a similar pattern of asymmetric IHTTs (i.e., faster left-to-right transfer, as discussed above). This result is inconsistent with the findings of the three previous studies (to our knowledge) that have used ERPs to investigate for IHTT abnormalities to unilaterally-presented visual stimuli in patients with SZ (Barnett et al., 2005; Barnett and Kirk, 2005; Endrass et al., 2002). Specifically, all three of these studies reported that while right-to-left transfer was faster than left-to-right in HCs, this asymmetry in IHTT was not present in schizophrenia patients. It should be noted, however, that there were substantial methodological differences between the present study and these three previous studies which could have contributed to the conflicting results.

Firstly, the present study estimated IHTT on the basis of P1 latency, in addition to N1 latency which was used in the aforementioned studies. The advantage of estimating IHTT on the basis of P1 latency is that the P1 represents an earlier stage of visual processing, likely to be closer to the point of initial interhemispheric transfer than the N1 (Saron and Davidson,

1989). The N1 reflects a later stage of visual processing that is sensitive to object categorization, unlike the P1 (e.g., Bentin et al., 1996). Furthermore, a recent study demonstrated that the hemispheric asymmetry of the N1 can reflect the relative rather than the retinotopic position of objects (Wascher et al., 2009). Thus, the P1 may be a better component with which to estimate IHTT than the N1.

Secondly, the present study estimated IHTTs on the basis of CSD transformed data. CSD is advantageous for the comparison of peak latencies in that it minimizes the effects of two established confounds, namely volume conduction (which causes component spread and overlap) and common reference (which results in the component latencies being influenced by the activity of the reference electrode (Saron et al., 2003)).

Thirdly, as per the study of (Endrass et al., 2002) but in contrast to the studies of (Barnett et al., 2005; Barnett and Kirk, 2005) the present study estimated IHTT from multiple posterior electrode pairs for both P1 and N1. These electrode pairs were chosen on the basis that they showed the largest component amplitudes to the visual stimuli at both the contralateral and ipsilateral electrode, and were thus anticipated to evince the most reliable peak latencies. Thus there are several potential methodological reasons why the results of the present study are different to the results of the three aforementioned studies.

No significant differences were observed between the schizophrenia and control participants in terms of either their FA or Mode in the visual fibers of the corpus callosum. Although this is the first DTI study (to our knowledge) that has specifically investigated for diffusion abnormalities in these particular fibers, the null result is consistent with the majority of studies that have investigated for diffusion abnormalities in primary sensorimotor fibers in schizophrenia patients in schizophrenia patients (e.g., Schneiderman et al., 2009; Shergill et al., 2007). In contrast, diffusion abnormalities in general, and FA abnormalities in particular, have consistently been observed in the white-matter fasciculi that either connect the frontal lobes (e.g., genu of the corpus callosum; Whitford et al., 2010b) or project from the frontal lobes, including the uncinate (Burns et al., 2003), arcuate (Phillips et al., 2009), superior longitudinal fasciculus (Karlsgodt et al., 2008) and cingulum (Kubicki et al., 2003). A recent meta-analysis by Ellison-Wright et al., (2009) of fifteen voxel-based DTI studies also reported evidence for abnormalities in frontally-projecting fasciculi in patients with schizophrenia. In contrast, however, while Kanaan et al. (2005) identified DTI abnormalities of some sort in 16 of the 19 studies analyzed, they did not identify a consistent pattern of abnormality, suggesting that while there is some evidence that the frontally-projecting fibers are preferentially affected in patients with schizophrenia, this point remains open to debate. Nevertheless, it is notable that in contrast to the primary sensorimotor fasciculi, which generally mature *in utero* or in early childhood, these frontally-projecting fasciculi are among the latest to structurally mature, with myelination typically continuing through adolescence and into early adulthood (Lebel et al., 2008; Schneiderman et al., 2009; Tamnes et al., 2010; Yakovlev et al., 1967). In light of the fact that adolescence/early adulthood is the most common age-of-onset for SZ, it has been proposed that abnormalities in these developmental processes of periadolescent myelination could represent a root cause of the disorder (Bartzokis, 2002).

The most significant finding of this paper was the discovery of an empirical relationship between IHTT – as quantified from the asymmetry in P1 latency at electrodes P9 and P10 – and the diffusion properties of the visual callosal fibers, as quantified with the diffusion metrics of FA and Mode. Specifically, the regression model – which accounted for 28.5% of the variance in IHTT – revealed that an increase of 10 ms in IHTT was associated with a decrease of approximately 0.035 in FA (i.e., more isotropic diffusion ellipsoids) and an increase of 0.14 in Mode (i.e., more prolate diffusion ellipsoids). Whilst the relationship

between Mode and white-matter integrity has not been well established – although a study by Kindlmann et al. (2007) found evidence that abnormally increased Mode was associated with abnormalities in crossing fibers – reductions in FA have consistently been associated with white-matter pathology, including in dysmyelinated mice (Harsan et al., 2006), and patients with the demyelinating disease multiple sclerosis (Roosendaal et al., 2009). Furthermore, such white-matter pathology has consistently been associated with slowed neural transmission velocity, for example in the slowed action potentials observed in dysmyelinated mice *in situ* (Roy et al., 2007), and in the increased P1 latencies to visually-evoked potentials typically observed in multiple sclerosis patients with optic neuritis (Jones, 1993). Hence our finding of a significant negative correlation between FA and IHTT (i.e., longer transmission times associated with lower FA and reduced white-matter integrity) is consistent with the available literature, and suggests that the established microscopic relationship between white-matter integrity and transmission velocity is observable at the macroscopic scale with neuroimaging. It should be acknowledged, however, that while transcallosal connections between the primary visual cortices have been identified in humans (Clarke and Miklossy, 1990; Saenz and Fine, 2010) and several other mammals including macaques (Kennedy et al., 1986), cats (Payne, 1991) and tree-shrews (Bosking et al., 2000), the extent and topographic organization of these callosal connections remains an ongoing topic of investigation in the neuroscience literature.

The observed relationship between FA/Mode and IHTT could also account for our failure to identify IHTT abnormalities in the schizophrenia patients, as the schizophrenia patients did not exhibit abnormalities in either FA or Mode in their visual corpus fibers. However, as mentioned previously, there are a number of fasciculi – particularly frontally-projecting fasciculi – in which SZ patients do show consistent and substantial diffusion abnormalities. Whilst there are significant differences between the microstructural properties of these frontally-projecting fasciculi and the visual callosum fibers investigated in the present study (e.g., Cherubini et al., 2009), if a similar relationship existed between transmission velocity and FA/Mode in these frontal fasciculi, then schizophrenia patients would be expected to experience significant conduction delays in signals traveling along these fasciculi. Such conduction delays could disrupt the precise temporal synchronization that is necessary for effective communication between discrete populations of oscillating neurons (Fries, 2005) which, in line with the 'connectivity' theories of SZ (Andreasen et al., 1999; Bartzokis, 2002; Bressler, 2003; Phillips and Silverstein, 2003), could underpin the cognitive disorganization characteristic of the disorder.

A limitation of the present study relates to the fact the most of the schizophrenia patients had been taking antipsychotic medications for several years. This is problematic in light of research indicating that antipsychotic medications (both typical and atypical) can influence brain structure and function in and of themselves (Konopaske et al., 2008). It should be reiterated that the schizophrenia patients in the present study did not exhibit abnormalities in either their IHTTs or in the diffusion properties of their visual corpus fibers, and furthermore did not show a differential relationship between FA/Mode and IHTT to that of the HCs. Nevertheless, it would be highly advantageous if the results of the present study could be replicated in a sample of neuroleptic-naïve SZ patients. It should also be acknowledged that the P9/P10 electrode pair, which was the site of the one significant IHTT/DTI correlation, does not lie directly over the end-points of the visual CC fibers extracted from the DTI data. Notwithstanding recent developments in high-density electrode setups, however, the spatial resolution of standard, scalp-recorded EEG is typically no better than several centimeters (Srinivasan et al., 1998). Given this technical limitation, it was not feasible to predict *a priori*, on the basis of their spatial locations, which electrode pair would provide the most reliable measure of IHTT. In light of this, we instead investigated for IHTT/DTI correlations in a battery of four electrode pairs, and subsequently performed a conservative correction for

multiple comparisons. That is, rather than an *a priori* selection based on their spatial locations, these four electrode pairs were selected *a posteriori* on the basis of the magnitude of their visual-evoked potentials. Finally, it should also be acknowledged that a number of longitudinal fasciculi pass close to the visual CC fibers, including the inferior longitudinal fasciculus and the inferior fronto-occipital fasciculus, and hence that possibility that some of the voxels defined by the labelmaps were influenced by crossing fibers cannot be discounted. However, given the fact that average Mode was highly positive (>.6) in these fibers, combined with the fact that Mode is typically sub-zero in voxels severely influenced by fiber crossings (Ennis and Kindlmann, 2006) suggests that the majority of voxels defined by labelmaps were not significantly influenced by crossing fibers.

In summary, the present study identified highly significant IHTTs to unilaterally-presented stimuli in both healthy individuals and chronic schizophrenia patients. IHTT (calculated from the P1 component) from left-to-right hemisphere was found to be significantly faster than from right-to-left hemisphere, across groups. The schizophrenia patients did not exhibit abnormalities in either the magnitude or asymmetry of their IHTTs, nor did they exhibit abnormalities in the diffusion properties (quantified with FA and Mode) of the visual fibers of the corpus callosum. However, linear regression indentified a significant relationship, in both groups, between IHTT and the diffusion properties of the visual callosum fibers, such that participants with the lowest FA and highest Mode exhibited the longest IHTTs. If such a relationship held in such frontally-projecting fasciculi – fasciculi that have consistently been found to be structurally abnormal in schizophrenia – this would imply the presence of conduction delays along these fibers in schizophrenia patients. Such conduction delays could potentially disrupt neural coherence, which could represent the neural basis of the 'cognitive dysmetria' that has been proposed to underlie the disease (Andreasen et al., 1999).

Acknowledgments

References

Andreasen N, Nopoulos P, O'Leary D, Miller D, Wassink T, Flaum M. Defining the phenotype of schizophrenia: cognitive dysmetria and its neural mechanisms. Biol Psychiatry 1999;46:908–920. [PubMed: 10509174]

Barnett K, Corballis M, Kirk I. Symmetry of callosal information transfer in schizophrenia: a preliminary study. Schizophr Res 2005;74:171–178. [PubMed: 15721997]

Barnett K, Kirk I. Lack of asymmetrical transfer for linguistic stimuli in schizophrenia: an ERP study. Clin Neurophysiol 2005;116:1019–1027. [PubMed: 15826841]

Bartzokis G. Schizophrenia: breakdown in the well-regulated lifelong process of brain development and maturation. Neuropsychopharmacology 2002;27:672–683. [PubMed: 12377404]

Basser PJ, Pierpaoli C. Microstructural and physiological features of tissues elucidated by quantitative-diffusion-tensor MRI. J Magn Reson B 1996;111:209–219. [PubMed: 8661285]

Baumann N, Pham-Dinh D. Biology of oligodendrocyte and myelin in the mammalian central nervous system. Physiol Rev 2001;81:871–927. [PubMed: 11274346]

Bayard S, Gosselin N, Robert M, Lassonde M. Inter- and intra-hemispheric processing of visual event-related potentials in the absence of the corpus callosum. J Cogn Neurosci 2004;16:401–414. [PubMed: 15072676]

Bentin S, Allison T, Puce A, Perez E, McCarthy G. Electrophysiological studies of face perception in humans. Journal of Cognitive Neuroscience 1996;8:551–565. [PubMed: 20740065]

Bosking WH, Kretz R, Pucak ML, Fitzpatrick D. Functional specificity of callosal connections in tree shrew striate cortex. J Neurosci 2000;20:2346–2359. [PubMed: 10704509]

Braun C. Estimation of interhemispheric dynamics from simple unimanual reaction time to extrafoveal stimuli. Neuropsychol Rev 1992;3:321–365. [PubMed: 1306109]

Bressler S. Cortical coordination dynamics and the disorganization syndrome in schizophrenia. Neuropsychopharmacology 2003;28(Suppl 1):S35–39. [PubMed: 12827142]

Brown W, Jeeves M. Bilateral visual field processing and evoked potential interhemispheric transmission time. Neuropsychologia 1993;31:1267–1281. [PubMed: 8127426]

Burns J, Job D, Bastin M, Whalley H, Macgillivray T, Johnstone E, Lawrie S. Structural disconnectivity in schizophrenia: a diffusion tensor magnetic resonance imaging study. Br J Psychiatry 2003;182:439–443. [PubMed: 12724248]

Cherubini A, Péran P, Hagberg G, Varsi A, Luccichenti G, Caltagirone C, Sabatini U, Spalletta G. Characterization of white matter fiber bundles with T2* relaxometry and diffusion tensor imaging. Magn Reson Med 2009;61:1066–1072. [PubMed: 19253372]

Cheung V, Cheung C, McAlonan G, Deng Y, Wong J, Yip L, Tai K, Khong P, Sham P, Chua S. A diffusion tensor imaging study of structural dysconnectivity in never-medicated, first-episode schizophrenia. Psychol Med 2008;38:877–885. [PubMed: 17949516]

Clarke S, Miklossy J. Occipital cortex in man: organization of callosal connections, related myelo- and cytoarchitecture, and putative boundaries of functional visual areas. J Comp Neurol 1990;298:188–214. [PubMed: 2212102]

Cook, Er; Miller, G. Digital filtering: background and tutorial for psychophysiologists. Psychophysiology 1992;29:350–367. [PubMed: 1626044]

Cuypers M, Dickson K, Pinckers A, Thijssen J, Hommes O. Discriminative power of visual evoked potential characteristics in multiple sclerosis. Doc Ophthalmol 1995;90:247–257. [PubMed: 8846733]

Ellison-Wright I, Bullmore E. Meta-analysis of diffusion tensor imaging studies in schizophrenia. Schizophr Res 2009;108:3–10. [PubMed: 19128945]

Endrass T, Mohr B, Rockstroh B. Reduced interhemispheric transmission in schizophrenia patients: evidence from event-related potentials. Neurosci Lett 2002;320:57–60. [PubMed: 11849763]

Ennis D, Kindlmann G. Orthogonal tensor invariants and the analysis of diffusion tensor magnetic resonance images. Magn Reson Med 2006;55:136–146. [PubMed: 16342267]

Fields R. White matter in learning, cognition and psychiatric disorders. Trends Neurosci 2008;31:361–370. [PubMed: 18538868]

First, M.; Spitzer, R.; Gibbon, M.; Williams, J. Structured Clinical Interview for DSM-IV® Axis I Disorders (SCID-I), Clinician Version. American Psychiatric Publishing, Inc; 1997.

First, MB.; Spitzer, RL.; Gibbon, M.; Williams, BJ. Structured Clinical Interview for DSM-IV-TR Axis I Disorders, Research Version, Non-patient Edition. (SCID-I/NP). Biometrics Research, New York State Psychiatric Institute; New York: 2002.

Foong J, Maier M, Clark C, Barker G, Miller D, Ron M. Neuropathological abnormalities of the corpus callosum in schizophrenia: a diffusion tensor imaging study. J Neurol Neurosurg Psychiatry 2000;68:242–244. [PubMed: 10644799]

Fries P. A mechanism for cognitive dynamics: neuronal communication through neuronal coherence. Trends Cogn Sci 2005;9:474–480. [PubMed: 16150631]

Friston K. The disconnection hypothesis. Schizophrenia Research 1998;30:115–125. [PubMed: 9549774]

Gasparotti R, Valsecchi P, Carletti F, Galluzzo A, Liserre R, Cesana B, Sacchetti E. Reduced fractional anisotropy of corpus callosum in first-contact, antipsychotic drug-naive patients with schizophrenia. Schizophr Res 2009;108:41–48. [PubMed: 19103476]

Harsan L, Poulet P, Guignard B, Steibel J, Parizel N, de Sousa P, Boehm N, Grucker D, Ghandour M. Brain dysmyelination and recovery assessment by noninvasive in vivo diffusion tensor magnetic resonance imaging. J Neurosci Res 2006;83:392–402. [PubMed: 16397901]

Hasan K. Diffusion tensor eigenvalues or both mean diffusivity and fractional anisotropy are required in quantitative clinical diffusion tensor MR reports: fractional anisotropy alone is not sufficient. Radiology 2006;239:611–612. author reply 612–613. [PubMed: 16641362]

Hollingshead, A. Two factor of index of social position. Yale Station; New Haven: 1965.

Jones S. Visual evoked potentials after optic neuritis. Effect of time interval, age and disease dissemination. J Neurol 1993;240:489–494. [PubMed: 8263555]

Kanaan R, Kim J, Kaufmann W, Pearlson G, Barker G, McGuire P. Diffusion tensor imaging in schizophrenia. Biol Psychiatry 2005;58:921–929. [PubMed: 16043134]

Kandel, ER.; Schwartz, JH.; Jessell, TM. Principles of neural science. McGraw Hill; New York: 2000.

Karlsgodt K, van Erp T, Poldrack R, Bearden C, Nuechterlein K, Cannon T. Diffusion tensor imaging of the superior longitudinal fasciculus and working memory in recent-onset schizophrenia. Biol Psychiatry 2008;63:512–518. [PubMed: 17720147]

Kayser J, Tenke C. Principal components analysis of Laplacian waveforms as a generic method for identifying ERP generator patterns: I. Evaluation with auditory oddball tasks. Clin Neurophysiol 2006;117:348–368. [PubMed: 16356767]

Kennedy H, Dehay C, Bullier J. Organization of the callosal connections of visual areas V1 and V2 in the macaque monkey. J Comp Neurol 1986;247:398–415. [PubMed: 3088065]

Kindlmann G, Ennis D, Whitaker R, Westin C. Diffusion tensor analysis with invariant gradients and rotation tangents. IEEE Trans Med Imaging 2007;26:1483–1499. [PubMed: 18041264]

Konopaske G, Dorph-Petersen K, Sweet R, Pierri J, Zhang W, Sampson A, Lewis D. Effect of chronic antipsychotic exposure on astrocyte and oligodendrocyte numbers in macaque monkeys. Biol Psychiatry 2008;63:759–765. [PubMed: 17945195]

Kubicki M, McCarley R, Westin C, Park H, Maier S, Kikinis R, Jolesz F, Shenton M. A review of diffusion tensor imaging studies in schizophrenia. J Psychiatr Res 2007;41:15–30. [PubMed: 16023676]

Kubicki M, Westin C, Nestor P, Wible C, Frumin M, Maier S, Kikinis R, Jolesz F, McCarley R, Shenton M. Cingulate fasciculus integrity disruption in schizophrenia: a magnetic resonance diffusion tensor imaging study. Biol Psychiatry 2003;54:1171–1180. [PubMed: 14643084]

Lebel C, Walker L, Leemans A, Phillips L, Beaulieu C. Microstructural maturation of the human brain from childhood to adulthood. Neuroimage 2008;40:1044–1055. [PubMed: 18295509]

Makeig, S.; Bell, AJ.; Jung, T-P.; Sejnowski, TJ. Independent component analysis of electroencephalographic data. In: Touretzky, DMM.; Hasselmo, M., editors. Advances in Neural Information Processing Systems. MIT Press; Cambridge, MA: 1996. p. 145-151.

Marzi C, Bisiacchi P, Nicoletti R. Is interhemispheric transfer of visuomotor information asymmetric? Evidence from a meta-analysis. Neuropsychologia 1991;29:1163–1177. [PubMed: 1838793]

Moes P, Brown W, Minnema M. Individual differences in interhemispheric transfer time (IHTT) as measured by event related potentials. Neuropsychologia 2007;45:2626–2630. [PubMed: 17499316]

Myers, R. Classical and modern regression with applications. 2. Duxbury; Boston, MA: 1990.

Nowicka A, Grabowska A, Fersten E. Interhemispheric transmission of information and functional asymmetry of the human brain. Neuropsychologia 1996;34:147–151. [PubMed: 8852877]

Oldfield RC. The assessment and analysis of handedness: the Edinburgh inventory. Neuropsychologia 1971;9:97–113. [PubMed: 5146491]

Oostenveld R, Praamstra P. The five percent electrode system for high-resolution EEG and ERP measurements. Clin Neurophysiol 2001;112:713–719. [PubMed: 11275545]

Patston L, Kirk I, Rolfe M, Corballis M, Tippett L. The unusual symmetry of musicians: musicians have equilateral interhemispheric transfer for visual information. Neuropsychologia 2007;45:2059–2065. [PubMed: 17374388]

Payne BR. Visual-field map in the transcallosal sending zone of area 17 in the cat. Vis Neurosci 1991;7:201–219. [PubMed: 1721530]

Perrin F, Bertrand O, Pernier J. Scalp current density mapping: value and estimation from potential data. IEEE Trans Biomed Eng 1987;34:283–288. [PubMed: 3504202]

Perrin F, Pernier J, Bertrand O, Echallier J. Spherical splines for scalp potential and current density mapping. Electroencephalogr Clin Neurophysiol 1989;72:184–187. [PubMed: 2464490]

Phillips O, Nuechterlein K, Clark K, Hamilton L, Asarnow R, Hageman N, Toga A, Narr K. Fiber tractography reveals disruption of temporal lobe white matter tracts in schizophrenia. Schizophr Res 2009;107:30–38. [PubMed: 19028423]

Phillips WA, Silverstein SM. Convergence of biological and psychological perspectives on cognitive coordination in schizophrenia. Behavioral & Brain Sciences 2003;26:65–82. [PubMed: 14598440]

Roosendaal S, Geurts J, Vrenken H, Hulst H, Cover K, Castelijns J, Pouwels P, Barkhof F. Regional DTI differences in multiple sclerosis patients. Neuroimage 2009;44:1397–1403. [PubMed: 19027076]

Roy K, Murtie J, El-Khodor B, Edgar N, Sardi S, Hooks B, Benoit-Marand M, Chen C, Moore H, O'Donnell P, Brunner D, Corfas G. Loss of erbB signaling in oligodendrocytes alters myelin and dopaminergic function, a potential mechanism for neuropsychiatric disorders. Proc Natl Acad Sci U S A 2007;104:8131–8136. [PubMed: 17483467]

Saenz M, Fine I. Topographic organization of V1 projections through the corpus callosum in humans. NeuroImage 2010;52:1224–1229. [PubMed: 20553894]

Saron C, Davidson R. Visual evoked potential measures of interhemispheric transfer time in humans. Behav Neurosci 1989;103:1115–1138. [PubMed: 2803556]

Saron, CD.; Foxe, JJ.; Simpson, GV.; Vaughan, HG. Interhemispheric visuomotor activation: spatiotemporal electrophysiology related to reaction time. In: Zaidal, EIM., editor. The parallel brain: the congitive neuroscience of the corpus callosum. MIT Press; Cambridge, MA: 2003.

Schneiderman J, Buchsbaum M, Haznedar M, Hazlett E, Brickman A, Shihabuddin L, Brand J, Torosjan Y, Newmark R, Canfield E, Tang C, Aronowitz J, Paul-Odouard R, Hof P. Age and diffusion tensor anisotropy in adolescent and adult patients with schizophrenia. Neuroimage 2009;45:662–671. [PubMed: 19168139]

Shergill S, Kanaan R, Chitnis X, O'Daly O, Jones D, Frangou S, Williams S, Howard R, Barker G, Murray R, McGuire P. A diffusion tensor imaging study of fasciculi in schizophrenia. Am J Psychiatry 2007;164:467–473. [PubMed: 17329472]

Spencer K, Nestor P, Niznikiewicz M, Salisbury D, Shenton M, McCarley R. Abnormal neural synchrony in schizophrenia. J Neurosci 2003;23:7407–7411. [PubMed: 12917376]

Srinivasan R, Tucker D, Murias M. Estimating the spatial nyquist of the human EEG. Behavioral Research Methods, Instruments, & Computers 1998;30:8–19.

Stephan K, Friston K, Frith C. Dysconnection in schizophrenia: from abnormal synaptic plasticity to failures of self-monitoring. Schizophr Bull 2009;35:509–527. [PubMed: 19155345]

Tamnes C, Ostby Y, Fjell A, Westlye L, Due-Tønnessen P, Walhovd K. Brain maturation in adolescence and young adulthood: regional age-related changes in cortical thickness and white matter volume and microstructure. Cereb Cortex 2010;20:534–548. [PubMed: 19520764]

Uranova N, Vostrikov V, Vikhreva O, Zimina I, Kolomeets N, Orlovskaya D. The role of oligodendrocyte pathology in schizophrenia. Int J Neuropsychopharmacol 2007;10:537–545. [PubMed: 17313698]

Wascher E, Hoffmann S, Sänger J, Grosjean M. Visuo-spatial processing and the N1 component of the ERP. Psychophysiology 2009;46:1270–1277. [PubMed: 19744158]

Westerhausen R, Kreuder F, Woerner W, Huster R, Smit C, Schweiger E, Wittling W. Interhemispheric transfer time and structural properties of the corpus callosum. Neurosci Lett 2006;409:140–145. [PubMed: 17034948]

Whitford TJ, Ford JM, Mathalon DH, Kubicki M, Shenton ME. Schizophrenia, myelination and delayed corollary discharges. Schizophrenia Bulletin. 2010a10.1093/schbul/sbq105

Whitford TJ, Grieve SM, Farrow TF, Gomes L, Brennan J, Harris AWF, Gordon E, Williams LM. Volumetric white matter abnormalities in first-episode schizophrenia: a longitudinal, tensorbased morphometry study. American Journal of Psychiatry 2007;164:1082–1089. [PubMed: 17606660]

Whitford TJ, Kubicki M, Schneiderman JS, O'Donnell LJ, King R, Alvarado JL, Khan U, Markant D, Nestor PG, Niznikiewicz M, McCarley RW, Westin CF, Shenton ME. Corpus callosum

abnormalities and their association with psychotic symptoms in patients with schizophrenia. Biological Psychiatry 2010b;68:70–77. [PubMed: 20494336]

Whitford, TJ.; Kubicki, M.; Shenton, ME. Structural neuroimaging of schizophrenia. In: Shenton, ME.; Turetsky, B., editors. Understanding Neuropsychiatric Disorders. Cambridge University Press; New York: in press

Wilkinson, G. The Wide Range Achievement Test - Revision 3. Jastak Association; Wilmington, DE: 1993.

Yakovlev, P.; Lecours, A.; Minkowski, A. Regional development of the brain early in life. Blackwell Scientific Publications; Boston, Massachusetts: 1967. The myelinogenetic cycles of regional maturation of the brain; p. 3-70.
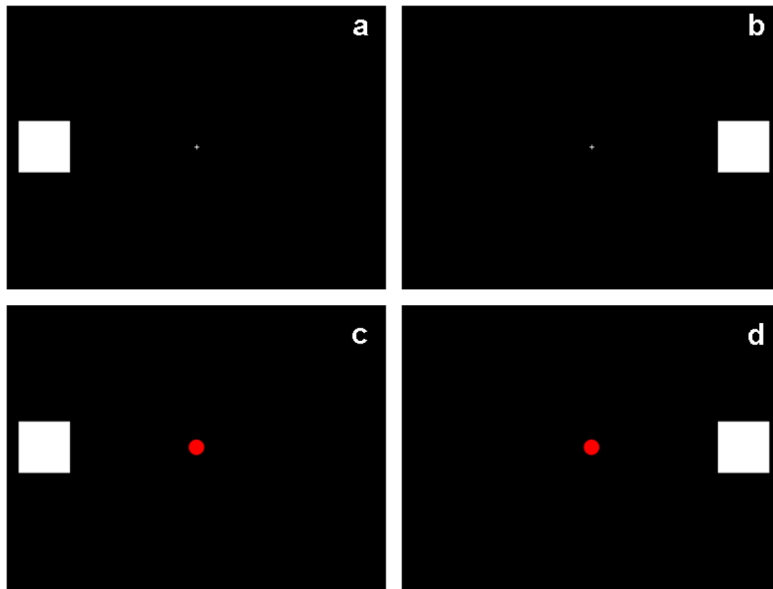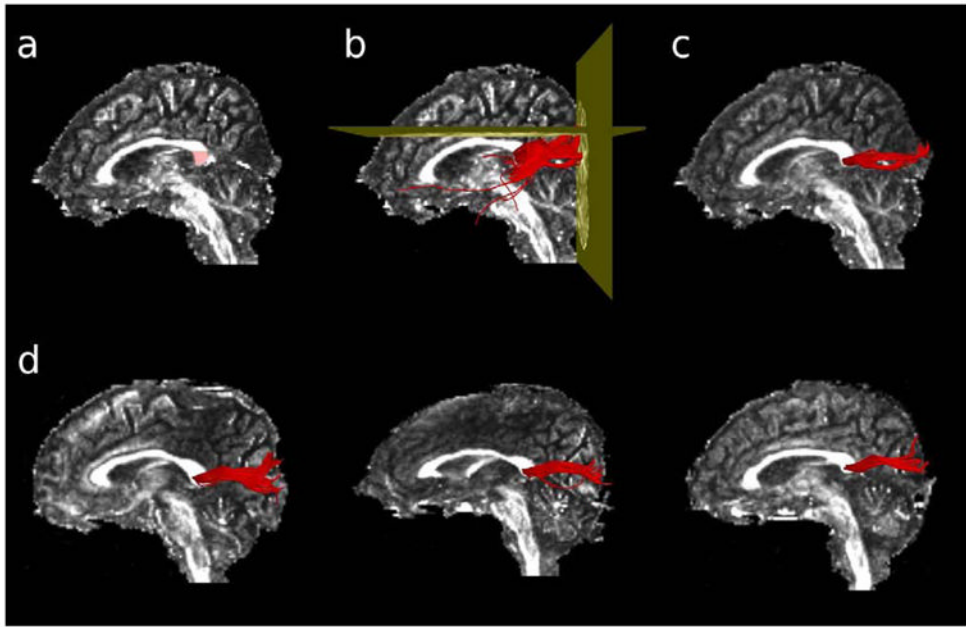
Figure 1.
Visual stimuli. The visual stimuli consisted of white squares (visual angle 2×2 degrees) presented on a black background for 82ms on the horizontal meridian, 6.79 degrees lateral to a central fixation cross. On target trials, the central fixation cross transformed into a red dot. 300 trials were presented, which delivered in 4 experimental blocks of 30 LVF non-target trials (panel a), 30 RVF non-target trials (panel b), 8 LVF target trials (panel c) and 7 RVF target trials (panel d), randomly presented. Participants were instructed to maintain their gaze on the central fixation cross and count the number of targets they saw.

## P1 electrode pairs
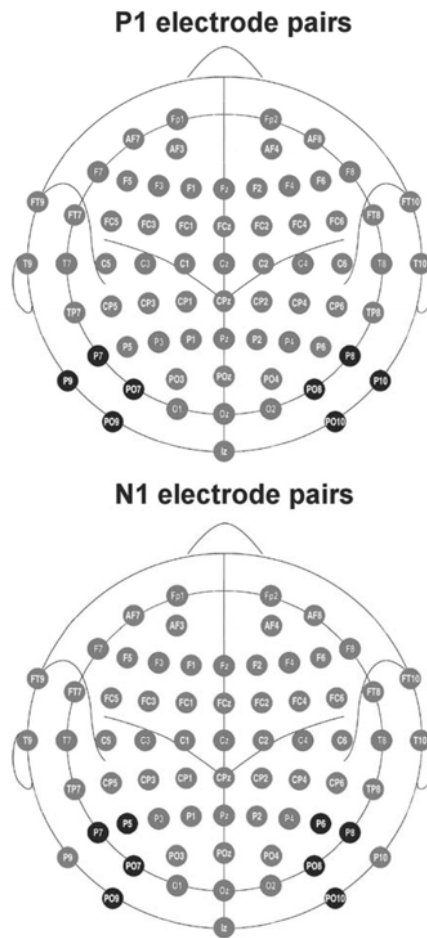
N1 electrode pairs

Figure 2.
A schematic of the electrode pairs, shaded in black, that were investigated in the analyses of the P1 (top) and N1 components (bottom) of the visually-evoked potentials, and from which inter-hemispheric transfer times (IHTTs) were subsequently calculated. The P1 component was measured from electrodes P7/P8, P9/P10, PO7/PO8 and PO9/PO10. The N1 component was measured from electrodes P5/P6, P7/P8, PO7/PO8 and PO9/PO10. These electrode pairs were chosen separately for each component on the basis that they showed the largest peak amplitudes to contralateral visual stimuli. Image modified from Oostenveld and Praamstra (2001).
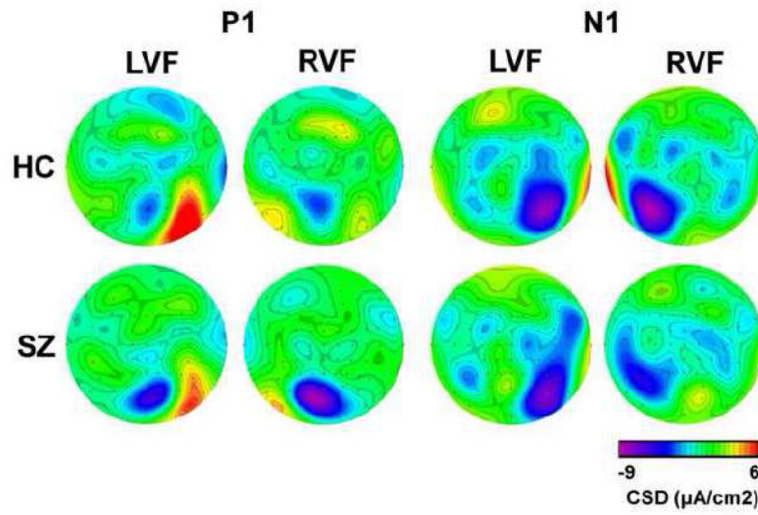
Figure 3.
Extraction of the visual fibers of the corpus callosum with DTI tractography. A region-of-interest was first manually drawn in the splenium of the corpus callosum, on the midsagittal slice of each participants' Fractional Anisotropy image (panel a). Voxels defined by the ROI were used as seedpoints for deterministic tractography. Fibers were excluded if they passed through the axial slice immediately dorsal to the corpus callosum, or if they failed to pass through the coronal slice defined by the posterior edge of the parieto-occipital fasciculus (panel b). The remaining fibers constituted the corpus fibers connecting the primary and secondary visual cortices bilaterally (panel c). Panel d shows the extracted visual corpus fibers for three representative individuals.
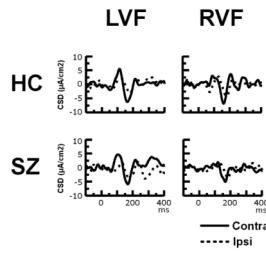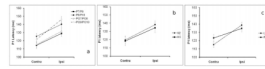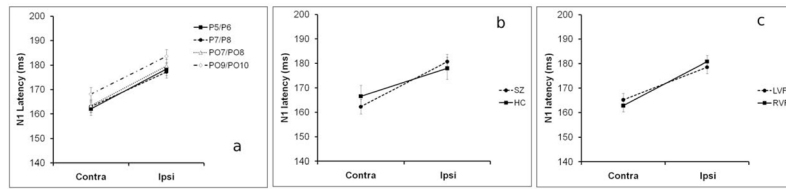
Figure 4.
Current Source Density Waveforms. Grand average CSD waveforms for contralateral (solid line) and ipsilateral (dotted line) visual stimuli presented in the left and right visual fields (LVF and RVF respectively) in 33 schizophrenia patients (SZ) and 20 healthy controls (HC) for the P7/P8 electrode pair. The solid line in the top left panel, for example, represents the ERP evoked at electrode P8 when a square was presented in the left visual field (i.e., the visual field contralateral to the electrode). The dotted line in the top left panel, in contrast, represents the ERP evoked at electrode P7 when a square was presented in the left visual field (i.e., the visual field ipsilateral to the electrode). The P7 and P8 electrode sites were chosen for display as they exhibited among the largest P1 and N1 amplitudes to both contralateral and ipsilateral stimuli.

Figure 5.
Current Source Density Headmaps. Axial headmaps (nasion at top) showing the topography of the CSD amplitude (μA/cm^2) of both the P1 and N1 components to left visual field (LVF) and right visual field (RVF) stimuli in 33 schizophrenia patients (SZ) and 20 healthy controls (HC).
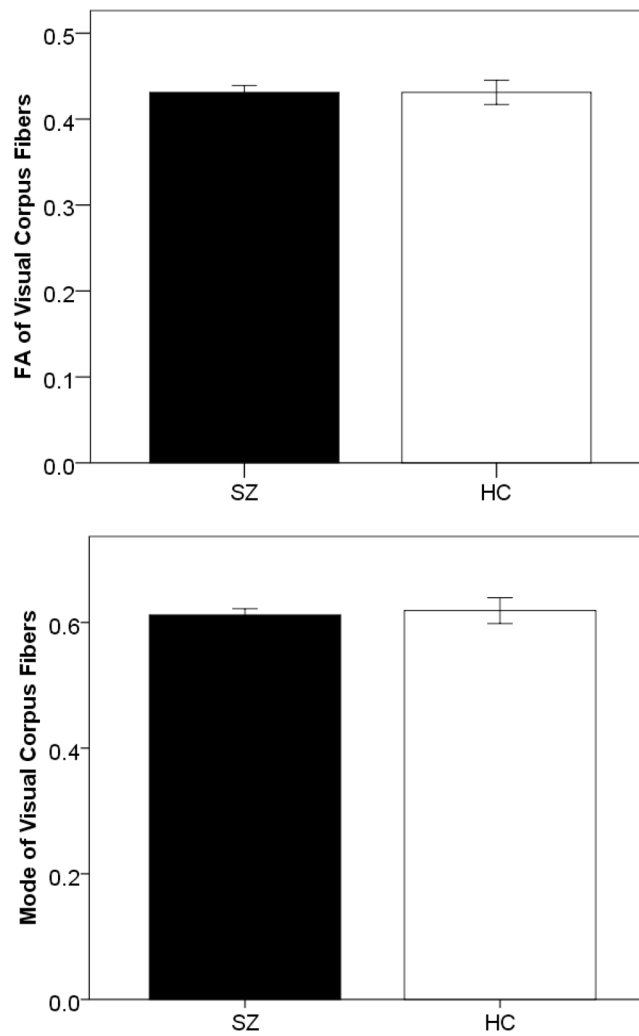
Figure 6.
P1 peak latencies to contralateral vs. ipsilateral visual stimuli. Panel (a) shows the P1 peak latencies to contralateral vs. ipsilateral stimuli for the four analyzed electrode pairs (P7/P8, P9/P10, PO7/PO8, PO9/PO10), across groups and visual fields. Panel (b) shows the P1 peak latencies to contralateral vs. ipsilateral stimuli for the SZ patients and healthy controls, across visual field and electrode pair. Panel (c) shows the P1 peak latencies to contralateral vs. ipsilateral stimuli for LVF and RVF stimuli, across group and electrode pair. Bars show the SEM.
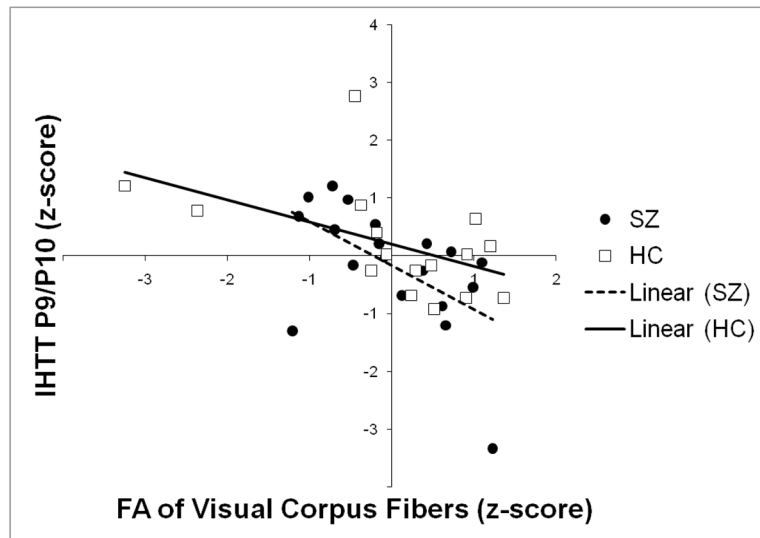
Figure 7.
N1 peak latencies to contralateral vs. ipsilateral visual stimuli. Panel (a) shows the N1 peak latencies to contralateral vs. ipsilateral stimuli for the four analyzed electrode pairs (P5/P6, P7/P8, PO7/PO8, PO9/PO10), across groups and visual fields. Panel (b) shows the N1 peak latencies to contralateral vs. ipsilateral stimuli for the SZ patients and healthy controls, across visual field and electrode pair. Panel (c) shows the N1 peak latencies to contralateral vs. ipsilateral stimuli for LVF and RVF stimuli, across group and electrode pair. Error bars show the SEM.

Figure 8.
Bar graphs showing between-group differences in Fractional Anisotropy (top) and Mode (bottom) for the 19 SZ patients (black bars) and 16 healthy controls (white bars) who underwent DTI scanning. Error bars show the SEM.

Figure 9.
Scatterplot showing the relationship between standardized FA (horizontal axis) and standardized IHTT (vertical axis; calculated from the P1 latency difference between electrodes P9 and P10) in the 19 SZ patients (black dots) and 16 healthy controls (white squares). The line-of-best fit for the SZ patients is shown as a dashed line and the line-of-best-fit for the healthy controls is shown as a solid line.

Table 1

Demographic details of those subjects who participated in the electroencephalography (EEG) and Diffusion-Tensor Imaging (DTI) components of the study.

a) EEG Component

Variable	Schizophrenia participants (n=33)			Healthy control participants (n=20)		
	Mean	SD	Range	Mean	SD	Range
Age (years)[1]	40.6	11.5	20–55	41.2	9.0	25–53
Gender[2]	29M, 4F			19M, 1F		
Handedness[3]	0.74	0.23	0.25–1	0.73	0.21	0.33–1
Premorbid IQ[4]	97.3	15.4	75–145	108	20.5	84–148
Parental socioeconomic status[5]	2.73	1.28	1–5	2.24	1.09	1–4
Age-of-Onset	23.6	5.9	16–38		-	
Medication dose (CPZ equivalents)	355	226	0–900		-	
PANSS-Positive	21.6	8.07	7–41		-	
PANSS-Negative	19.4	8.80	7–38		-	
PANSS-General	38.0	13.8	16–74		-	

b) DTI Component

Variable	Schizophrenia participants (n=19)			Healthy control participants (n=16)		
	Mean	SD	Range	Mean	SD	Range
Age (years)[6]	43.7	9.8	22–55	43.0	8.0	28–53
Gender[7]	18M, 1F			16M		
Handedness[8]	0.75	0.23	0.25–1	0.73	0.22	0.33–1
Premorbid IQ[9]	98.5	14.7	75–145	108.9	21.4	84–148
Parental socioeconomic status[10]	2.41	1.06	1–4	2.21	1.12	1–4
Age-of-Onset	24.2	6.34	16–38		-	
Medication dose (CPZ equivalents)	320	243	0–900		-	
PANSS-Positive	22.8	7.8	7–41		-	
PANSS-Negative	19.1	7.8	7–37		-	

b) DTI Component

Variable	Schizophrenia participants (n=19)			Healthy control participants (n=16)		
	Mean	**SD**	**Range**	**Mean**	**SD**	**Range**
PANSS-General	39.6	13.9	20–74		-	

[1] HCvsSZ, p=.87,

[2] HCvsSZ, p=.82,

[3] HCvsSZ, p=.89

[4] HCvsSZ, p=.09,

[5] HCvsSZ, p=.20

[6] HCvsSZ, p=.82,

[7] HCvsSZ, p=.90,

[8] HCvsSZ, p=.87

[9] HCvsSZ, p=.13,

[10] HCvsSZ, p=.62